

การศึกษานาโนอินเดนเตชันและไมโครสแควชของไททาเนียมไดออกไซด์ฟิล์มที่มีโครงสร้างในระดับนาโน: การศึกษาผลกระทบของการหมุนของชั้นฐานรอง

นุโรจน์ พานิช¹ Naing Naing Aung² และ Sun Yong²

Nanyang Technological University, Singapore 639798

รับเมื่อ 21 มกราคม 2548 ตอรับเมื่อ 16 มีนาคม 2548

บทคัดย่อ

ไททาเนียมไดออกไซด์ฟิล์มที่มีโครงสร้างในระดับนาโนหนาถึง 2.65 ไมครอน ถูกเคลือบบนฐานรองเหล็กกล้าความเร็วสูง โดยใช้เครื่องสปีดเตอรัริงแบบแมกเนตรอน งานวิจัยนี้ได้พยายามในการเพิ่มสมบัติของความแข็งและเหนียวของฟิล์ม โดยการศึกษาการหมุนของชั้นฐานรองระหว่างการเคลือบเฟสและการจัดเรียงตัวของผลึกโดยใช้เทคนิคการเลี้ยวเบนของรังสีเอ็กซ์ ศึกษาโครงสร้างจุลภาคของแผ่นฟิล์มด้วยกล้องจุลทรรศน์อิเล็กตรอนแบบส่องกวาด ศึกษาสมบัติเชิงกลด้วยวิธีนาโนอินเดนเตชัน และศึกษาแรงยึดเหนี่ยวกันระหว่างแผ่นฟิล์มกับชั้นงานที่ถูกเคลือบด้วยไมโครสแควช ซึ่งจากผลการทดลองพบว่า กรณีไม่หมุนชั้นฐานรองระหว่างการเคลือบจะเพิ่มคุณสมบัติของความแข็งและเหนียวของฟิล์ม เนื่องจากฟิล์มมีความหนาชั้น เฟส (001) เพิ่มมากขึ้น ขนาดของเกรนเล็กกลง และความหนาแน่นของฟิล์มเพิ่มมากขึ้น

คำสำคัญ : ไททาเนียมไดออกไซด์ / เครื่องสปีดเตอรัริงแบบแมกเนตรอน / ความแข็ง / การยึดเกาะ / นาโนอินเดนเตชัน / ไมโครสแควช

¹ นักศึกษาระดับบัณฑิตศึกษา คณะวิศวกรรมศาสตร์

² ศาสตราจารย์ คณะวิศวกรรมศาสตร์

Nanoindentation and Microscratch Studies of Nanostructured Titanium Diboride Coatings: Effect of Substrate Rotation

Nurot Panich ^{1*}, Naing Naing Aung ², and Sun Yong ²

Nanyang Technological University, Singapore 639798

Received 21 January 2005 ; accepted 16 March 2005

Abstract

Titanium diboride (TiB₂) based nanostructured coatings up to 2.65 μm thick were deposited on high-speed steel by using magnetron sputtering technique. In order to achieve an extra hard and tough coating, effects of substrate rotation during deposition were thoroughly studied. X-ray diffraction (XRD) and field emission scanning electron microscopy (FESEM) were used to examine the phase and structure, respectively. Nanoindentation and microscratch test were conducted for mechanical characterisation and coating adhesion examination, respectively. It was found that without substrate rotation, the adhesion, hardness and modulus have been improved tremendously due to the enhancement of coating thickness, the promotion of the (001) orientation, the decrease of average grain size, and the increase in coating density.

Keywords : Titanium Diboride / Magnetron Sputtering / Hardness / Adhesion / Nanoindentation Test / Microscratch

¹ Graduate Student, School of Materials Engineering.

² Professor, School of Materials Engineering.

* Corresponding author Fax: (65) 6790-9081; E-mail: panich@pmail.ntu.edu.sg

1. Introduction

Hard coatings have been playing an important role for wear-resistance, tribological and armor-barrier applications because they show the promising and extraordinary performance to resist wear, as well as withstand severe impact and high pressure. Generally, TiB_2 based coating is one of the most widely studied as a hard material, which is able to apply for wear resistant application particularly under condition of high temperature (due to its low thermal expansion coefficient) [1]. However, a high hardness seems not to be enough for wear resistant application, as it is well known that the wear resistance is influenced by many other factors such as, coating thickness, friction coefficient, coating adhesion strength, toughness, etc. Unfortunately, the fact is that pure TiB_2 coatings are very brittle for direct use as a wear-resistant coating and the adhesion of TiB_2 coatings to substrate is rather poor.

Recently, many attempts have been studied for improving both adhesion and mechanical properties of coating, for example introducing sputter cleaning [2-4], applying substrate bias during deposition [5-7] and including deposition at a higher chamber pressure [3]. There is convincing that hardness and modulus were significantly increased when substrate bias (substrate plasma cleaning) is introduced before deposition. This improvement is explained by the beneficial enhancement of interface cleaning by removing oxides and residual contaminants at the substrate surface, which resulted in increasing coating's capability to distribute stress without brittle fracture during impact mechanism. However, at a fixed power, too much substrate cleaning power is shown to decrease the hardness and adhesion because the impurities from the deposition chamber may be sputtered and then deposited onto the substrate surface [8]. Although applying substrate bias during deposition helps to improve adhesion and mechanical properties due to increase of adatom mobility and ion bombardment, it may cause a residual stress at the interfacial area, which impairs the adhesion and mechanical properties.

At a low chamber pressure, it is easy to promote the collision of ions at the substrate surface, which conducts to a higher residual stress. Increasing the chamber pressure decreases the mean free path of the ions moving from the target to the substrate surface, where deposition occurs [3]. However, it is not easy to find an appropriate chamber pressure for a certain deposition. Another candidate method to improve coating properties is to control the deposition process by focusing on substrate rotation effect. In the case of having substrate rotation, generally during deposition the substrate is rotated to be near and far away from target. It is well-known that the sputtering rate decreases as the distance from the target increases. This indicates that the highest rate of sputtering occurs at the fixed position where the substrate is nearest to the target; and fixing the substrate

during deposition at this stationary point may be most beneficial to enhancing the coating properties. In addition, since the sputtering yield is very sensitive to the angle of incidence of the bombarding ion, the nearest to target which the angle is mostly 90° , may provide the most effective deposition.

In this study, in order to study in the effect of substrate rotation specifically, it is noted that there is no substrate cleaning and bias applied before and during deposition. The effect of substrate rotation is an only choice to investigate for enhancing coating adhesion as well as mechanical properties. It was found that without substrate rotation, the coating thickness is increased and the adhesion and mechanical properties, such as hardness and modulus have been improved tremendously.

2. Experiment

In this study, high-speed steel, HSS, (SECO WKE45, Sweden) with fully hardened and tempered condition was chosen as a substrate. HSS was cut into 12 mm × 12 mm × 3 mm pieces. The surface of specimen was prepared by grinding and polishing and then ultrasonic cleaning by acetone and ethanol respectively, before charging into the deposition chamber. Before deposition, all target were sputtered for cleaning for 20 min. A thin (about 50 nm) pure Ti interlayer was deposited first in all cases, by sputtering the Ti target for 10 minutes with a DC power of 200 W. This was followed by sputtering of the two TiB_2 targets for 3 hours with a rf power of 200 W for both sample 1 (substrate rotation) and sample 2 (no substrate rotation). The coating parameters are given in Table 1 and the deposition set up is schematically shown in Fig. 1.

The phase composition of the resultant coatings was examined by Rigagu X-ray diffractometer with $Cu-K\alpha$ radiation. Crystallographic phases were analysed by comparing the experimental diffraction patterns with the standard JCPDS data. The morphology of surfaces and fractured cross-sections of the coatings were imaged using a field emission scanning electron microscope (FESEM), Jeol JSM 6340F. A tungsten tip was heated and a 5 kV accelerating voltage was applied to release electrons in the SEM measurements. The emission current was 12 mA during operating and the working distance was about 8 mm. Coating thickness was examined by ball crater (Calotest). A stainless steel ball of 24.5 mm diameter was used for cratering with speed of 500 rpm for 240 s.

The scratch tracks and EDS mapping were investigated by SEM.

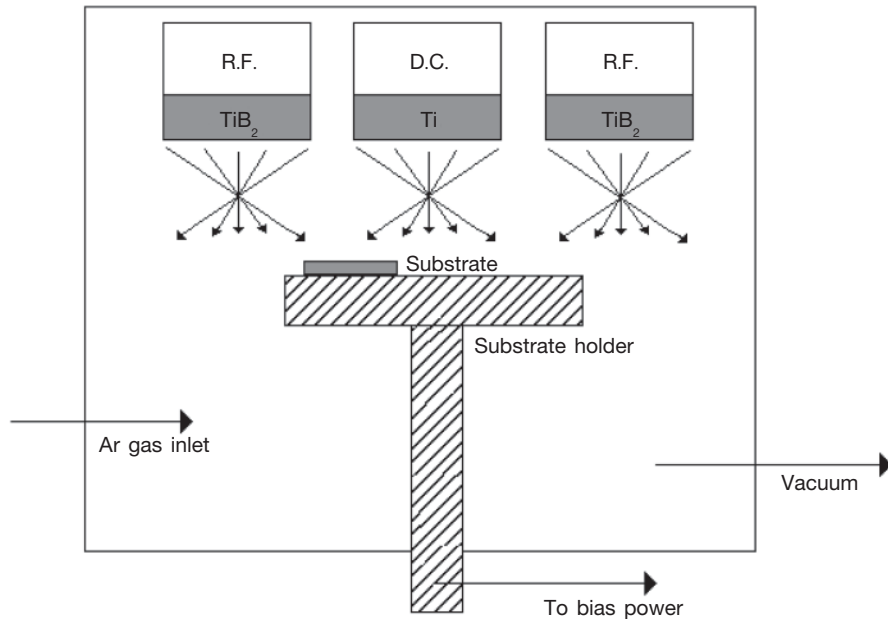


Fig. 1 The deposition set up in this study.

Table 1 Deposition conditions.

Substrate temperature	400 °C
Substrate-to-target distance	
TiB_2 Target	6 cm
Ti Target	10 cm
Gas	Ar
Total gas flow rate	20 sccm
Base pressure	5×10^{-4} Pa
Sputtering pressure	0.65 Pa
Substrate holder	2 rpm for sample 1 & stationary for sample 2
DC sputtering power	200 W
RF sputtering power	200 W
Deposition time	3 hours

Nanoindentation test was performed using the NanoTestTM (Micro Materials Limited, UK), with a Berkovich diamond indenter. All experiments were performed at a constant loading and unloading rate of 0.05 mN/s and to a penetration depth from 25 to 500 nm. The unloading curves were used to derive the hardness and reduced modulus values by the analytical technique developed by Oliver and Pharr [9].

The micro-scratch test was performed using the multipass wear test mode available in the NanoTest™ device with an indenter topped with a conical with spherical end form of 25 μm in radius. The stylus was tangentially moved to the surface at a speed 5 $\mu\text{m/s}$ over a length of 2,500 μm . After an initial 300 μm pre-scan under a small load of 0.25 mN, testing load was applied to the indenter with a linearly increasing load of 5 mN/s. For each scratch test, a set of surface profile along the track was measured i.e. firstly, the track profile before scratch (BS) by measuring the surface profile across full length of measured distance (2,500 μm) with the small load of 0.25 mN, secondly, during scratch (DS) by measuring the surface profile after BS step with increasing load after pre-scan length, and lastly, after scratch (AS) by measuring the surface profile track after DS step. Furthermore, the difference between BS and DS indicates the total scratch depth including elastic-plastic deformation and surface damage during scratch process [10]. The difference between BS and AS represents the depth of the scratch groove remaining on the sample surface after scratch tests. The critical load for coating failure (L_c), coatings adhesion strength, coefficient of friction and variation of properties with depth can be determined under micro-scratch test.

3. Results and discussion

3.1 Structural characterization of resultant coatings

Fig. 2 shows the XRD patterns of sample 1 and sample 2. XRD reveals broad peaks with a hexagonal structure. The broadness of the peaks indicates the nanocrystalline nature of the coating structure, as further confirmed by FESEM. From Fig. 2, it is noticed that sample 1 shows four broad peaks of (001), (100), (101) and (111) planes, which is typical achieving in TiB_2 deposition. Furthermore, it is noted that with deposition of TiB_2 without substrate rotation (sample 2), the intensity of peak (001) increases greatly and the intensity of peak (111) also increases, whilst the intensity of peak (100) and (101) decrease until almost disappeared. This may account for the observed increase in hardness because it is a well-known fact that TiB_2 coatings with (001) orientation yield the highest hardness as compared with TiB_2 coatings with other orientations [11]. Since the (001) orientation is known to yield the highest hardness, the hardness of sample 2 is expected to be higher than sample 1, as confirmed by nanoindentation test discussed later.

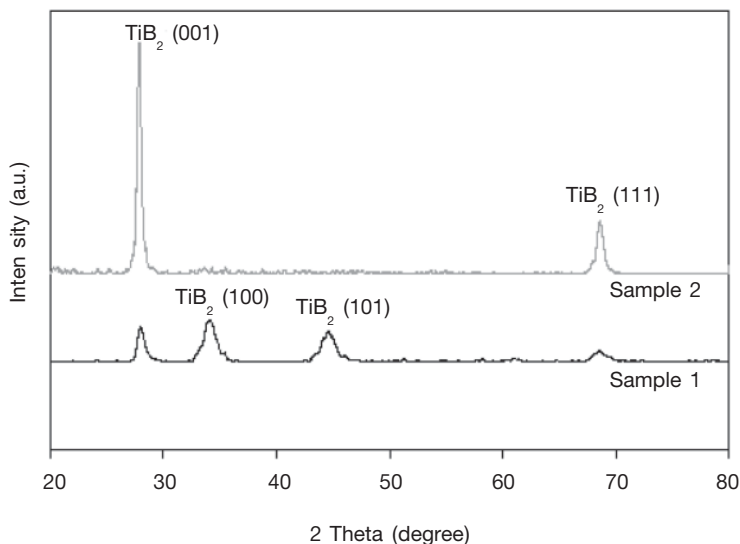


Fig. 2 XRD patterns of TiB_2 coatings.

The morphology and cross-section of both coating surfaces was examined under FESEM as shown in Fig. 3. Many grains have well-defined boundaries with the others as a rounded shape. Some porosity could be observed at grain boundaries. It also can be seen that the size of the grains is in nanometer scale, typically less than 20 nm in all dimensions (Fig. 3(a)). In addition, it can be seen that the surface roughness is not smooth due to the difference ion incidence angle during deposition of rotated sample. Some grains are bigger than others, which cause the heterogeneous properties for this sample due to the random deposition resulted in random orientation, as confirmed in Fig. 2 (sample 1). Sample 1 exhibit a columnar structure in the cross section (Fig. 3(b)).

For sample 2, the size of the grains also is in nanometer scale, typically also less than 20 nm in all dimensions, which are less porous and thus indicates improvement in film quality by the absence of substrate rotation during deposition ((Fig. 3(e)). It is noted that a dense coating texture (Fig. 3 (d)) was developed instead of a columnar structure. In addition, it can be seen that the surface roughness is much smoother due to the minimum of difference ion incidence angle during deposition of this sample. The ion incidence angle was manipulated to be controlled since the sputtering yield is very sensitive to the angle of incidence of the bombarding ion, at the nearest to target should provide the angle mostly near to 90° , which may provide the most effective deposition and most ordering atom arrangement. For this reason, the preferred (001) orientation is possibly promoted significantly, as shown in Fig. 2 (sample 2).

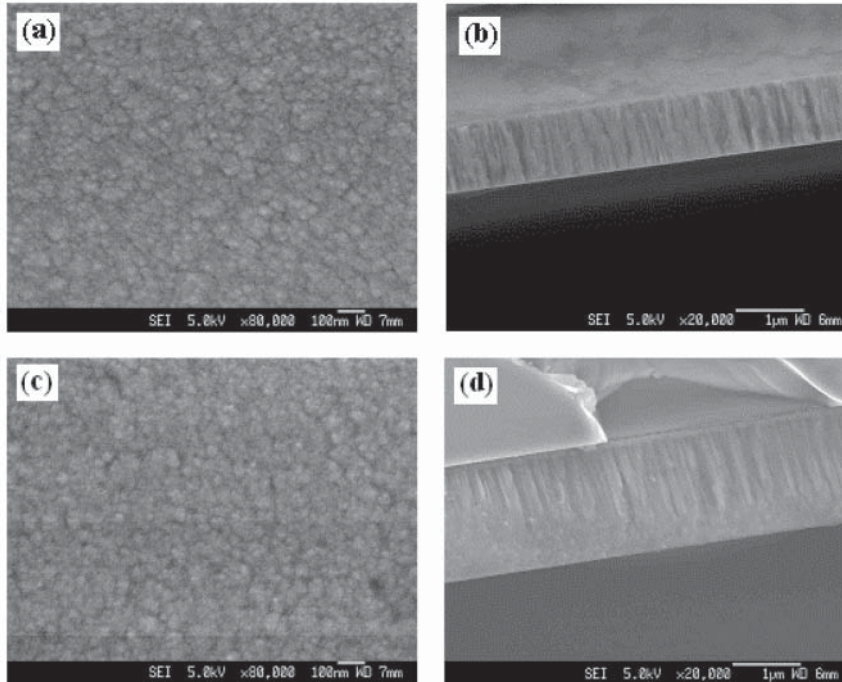


Fig. 3 FESEM images showing the surface morphology of sample 1 (a & b) and sample 2 (c & d).

3.2 Nanoindentation test

Ball crater reveals the coating thickness as shown in Table 2. It is noted that without substrate rotation, the coating thickness is increased from 1,350 nm to 2,650 nm. It indicates that the absence of substrate rotation at the fixed point nearest to the target can help to increase the coating thickness tremendously; in this work the increment is double.

Table 2 Properties of resultant coatings.

Materials	Substrate rotation	Coating thickness (micron)	Hardness (GPa)	Reduced modulus (GPa)	Critical load L _c (mN)	Yield load L _y (mN)
Sample 1	Rotated	1.35	25.3 ± 1.8	247.1 ± 14.6	528.3	135.6
Sample 2	Fixed	2.65	45.2 ± 1.2	368.2 ± 8.2	2,153.6	920.4

In order to assess the intrinsic mechanical properties of the coatings i.e. hardness and modulus, all specimens were tested at 90 nm penetration depth (less than 10% of coating thickness) in order to avoid the effect from substrate during indentation process. The hardness and modulus values measured by nanoindentation of sample 1 and sample 2 are summarised in Table 2.

Fig. 4 shows the load-displacement curves extracted at the penetration depth of 90 nm. The responses are typical of a hard material. For both samples, the loading curve is approximately parabolic as well as unloading one. This indicates that the elastic strains during indentation are large compared with the plastic strains which resulted in a good elastic recovery, in particular sample 2 (no substrate rotation), which shows the higher hardness and modulus.

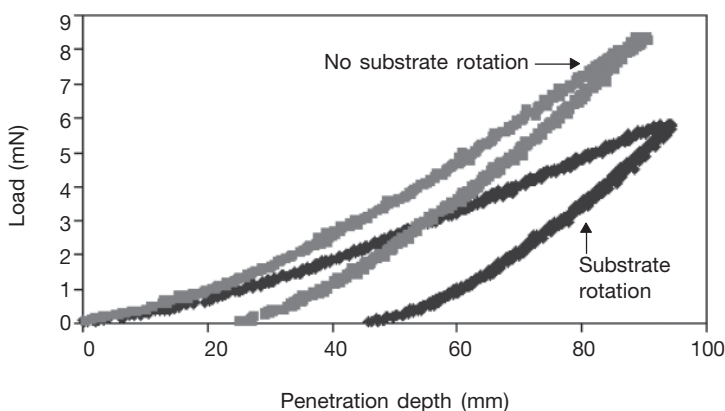


Fig. 4 Load-displacement curves extracted at the penetration depth of 90 nm.

Fig. 5 shows the results of hardness and reduced modulus measurements at various penetrations depth from 25 nm to 500 nm. It can be seen that at small penetration depths, the hardness tends towards a value of about 28 GPa and 45 GPa for sample 1 and sample 2, respectively (presumably the intrinsic hardness of coatings). However, at larger depths, the hardness decreases significantly, consistent with a substrate hardness of 12 GPa, which is considered a soft substrate compared to its coating.

This genuinely indicates the effect of substrate at a certain penetration depth. It is noted that the hardness of sample 2 (without substrate rotation) tends to have a stable hardness value (about 45 GPa) due to the thicker coating compared with sample 1. For sample 1, the hardness drops until the penetration depth reaches about 375 nm due to the substrate effect for the coating system. This may be able to estimate the coating thickness by nanoindentation measurement since the substrate could influence the coating hardness at 10% of coating thickness for the hard coating. Reduced modulus also shows a same trend as hardness.

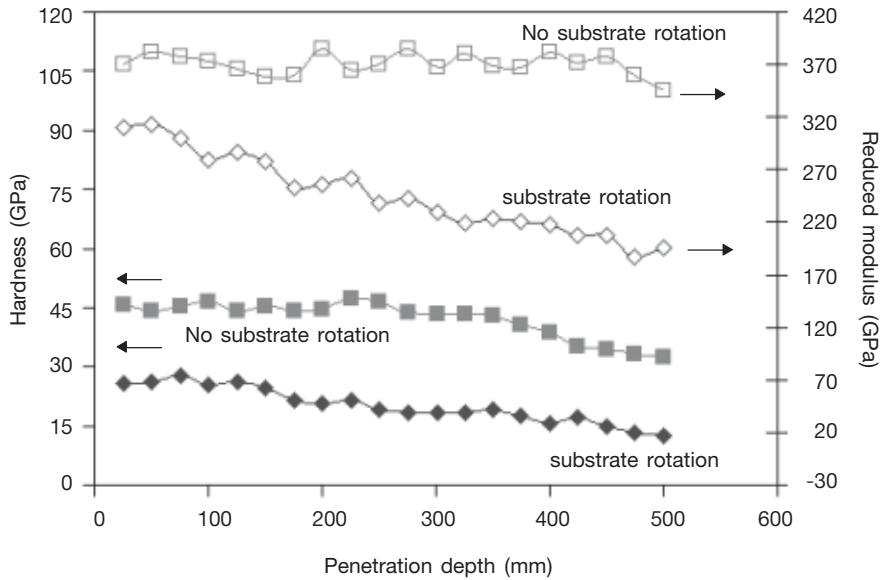


Fig. 5 Hardness and reduced modulus of resultant coatings at various penetration depths.

3.3 Microscratch test

Fig. 6 shows the microscratch curves with linearly increasing load of sample 2 (no substrate rotation). It can be seen that DS profile during scratch increases linearly with increasing load. The profiles in Fig. 6 can be divided into three regions. Firstly, the region from A to B demonstrates the pre-scan (300 mm) under the small load of 0.25 mN, where no scratch damage taken place, since BS, DS and AS have the same profile. Secondly, in the region from B to C, DS profile increases approximately linearly with increasing load. However, there is no plastic deformation or material loss in this period, which is shown by the elastic recovery of TiB_2 coating represented by AS and BS having the same profile.

It is noted that after point C, plastic deformation or material loss starts. In addition, the load at point C is crucial because it is a maximum load which coatings could be elastically recovered, which is called “yield load (L_y)”.

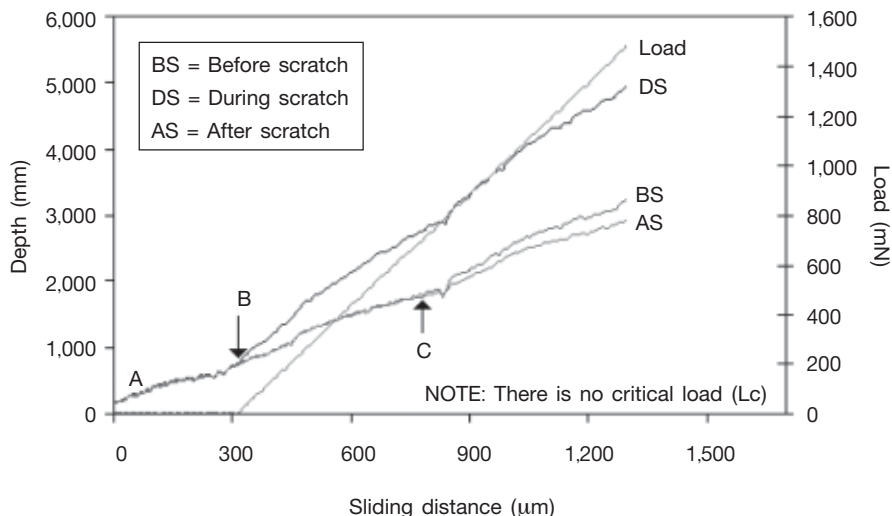


Fig. 6 Microscratch curves of deposited TiB_2 on sample 2.

As expected, it is noted that the distance of BC of sample 2 is much longer than sample 1 (not shown), which resulted from the increase of the yield load (L_Y). It indicates that deposition without substrate rotation enhances the coating strength, which resulted in coating elastic recovery. The L_Y values for both samples 1 and 2 are listed in Table 2. From Table 2, it is noted that deposition without substrate rotation shows the increment of L_Y values tremendously. It implies that deposition without substrate rotation helps significantly to extend the limitation of elastic recovery, which resulted in improving coating adhesion strength. It is noticed that there is no fluctuation in all profiles for sample 1 which indicates that there is no critical load point or materials lost at sliding distance 1,300 micron.

Fig. 7 demonstrates the typical scratch friction force curves with linearly increasing load (maximum load is 2,500 mN) for a TiB_2 coating of sample 1 (substrate rotation) and sample 2 (no substrate rotation). For sample 1 (substrate rotation), it can be seen that the polishing stage by the indenter is short ($L_c = 528.3$ mN), whilst the coating break-down or scratching the substrate is long until reaching the complete coating removal point (at 2,500 micron).

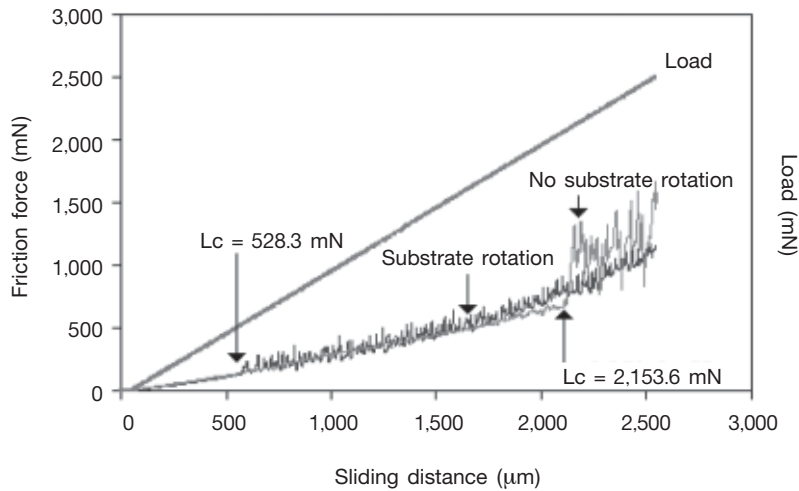


Fig. 7 Friction force curves of deposited TiB_2 coating under linearly increasing load.

On the other hand, sample 2 (no substrate rotation) shows a much longer polishing stage at L_c of 2,153.6 mN. Indeed, this indicates the strength of deposition without substrate rotation, resulted in a thicker coating and denser coating texture, which is beneficial to a better coating adhesion and is more suitable for use in tribological applications. The L_c values for both samples 1 and 2 are also listed in Table 2. It can be seen that L_c could be enhanced by deposition without substrate rotation as expected due to the significant increment of L_y .

3.4 SEM and EDS

In order to confirm the result of scratch test, SEM images and EDS mapping images of the scratch track were acquired. SEM and mapping images reveal the adhesive failure behaviour of the coatings at the critical load (L_c).

SEM reveals a typical scratch behaviour of TiB_2 coating (sample 1) (Fig. 8 (a)). The behaviour is consistent with poor adhesion due to weak interface bonding. It is obvious that the critical load (L_c) value is low (528.3 mN) and a massive coating delaminated along edges, which multiple coating cracking and chipping within scratch track can be observed after the L_c . In order to verify that the coating was removed from the substrate after the L_c , EDS mapping was used to identify the scratch marks quantitatively. Fig. 8 (b) shows the typical mapping, which can identify titanium (Ti), represented by white dots. It is noted that there is no Ti at the scratch track after L_c , which means there is no more coating at the scratch track after L_c as well. Fig. 8 (c) also proves that after L_c , HSS substrate representative by Fe can be found at the scratch track (white dot). From this result, it is noted that after failure starts at L_c the coating will be removed permanently along the scratch track.

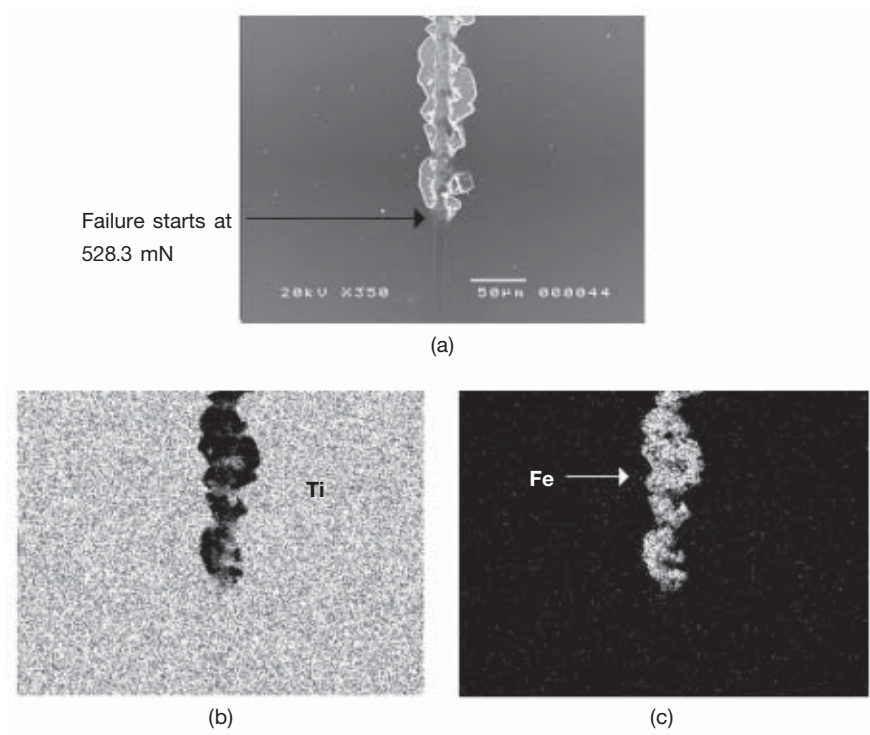


Fig. 8 (a) SEM of damage region and (b) & (c) EDS of the damage area illustrating sample 1.

For sample 2, without substrate rotation, Fig. 9 (a) shows that the coating is not completely removed until the critical load, and it is obvious that the critical load value is high (2,153.6 mN). In order to confirm that the coating was removed from the substrate, EDS mapping shows the distribution of Ti (the white dots) in the scratch track and coating surface. Obviously, there is no remaining Ti in the scratch track after a certain critical scratch load, which means that the coating was already removed. Fig. 9 (c) also proves that after L_c , Fe can be found at the scratch track (white dot), which Fe is representative HSS substrate. Furthermore, it is noted that the scratch width at the L_c is around 10 micron for sample 1 and around 35 micron for sample 2.

In order to identify the failure modes of the coatings, it was found that compressive spallation occurs in sample 1 and sample 2. However, Fig. 9 (a) shows that some parts of coating still remain at the side of the scratch track, which indicates the improvement of coating adhesion strength in sample 2. This indicates that the coating strength can be improved by deposition without rotating the substrate.

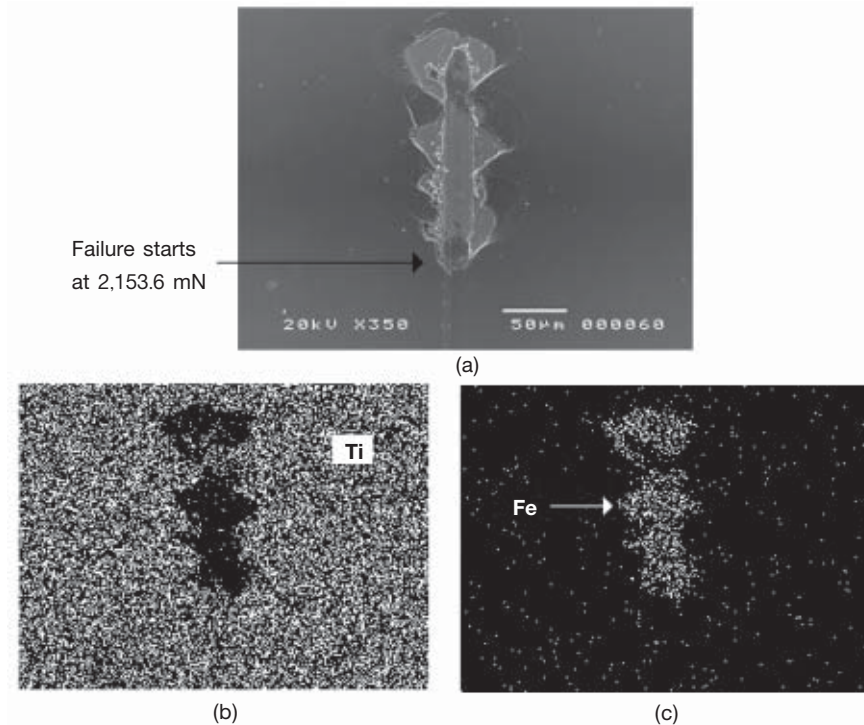


Fig. 9 (a) SEM of damage region and (b) & (c) EDS of the damage area illustrating sample 2.

4. Conclusions

(1) It was found that without substrate rotation, the adhesion, hardness and modulus have been improved tremendously due to the increase of coating thickness and the promotion of the (001) orientation.

(2) Under stationary deposition, a dense coating texture was developed instead of a columnar structure.

5. Acknowledgements

The research was supported by School of Materials Engineering, Nanyang Technological University, Singapore.

6. References

1. Kelesoglu E. and Mitterer, C., 1998, "Structure and Properties of TiB_2 Based Coatings Prepared by Unbalanced DC Magnetron Sputtering", *Surface Coatings and Technology*, Vol. 98, pp. 1483-1489.

2. Eryilmaz, O. L., Ürgen, M., Çakır, A. F., Kazmanlı M. K., and Kahraman, U. H., 1997, "The Effect of the Sputter Cleaning of Steel Substrates with Neutral Molecule Source on the Adhesion of TiN Films", *Surface Coatings and Technology*, Vol. 97, pp. 488-491.
3. Zhang, S., Xie, H., Hing, P., and Mo, Z., 1999, "Adhesion and Raman Studies of Magnetron Sputtered Amorphous Carbon on WC/Co", *Surface Engineering*, Vol. 15, No. 4, pp. 341-346.
4. Panich, N. and Sun, Y., 2004, "Microscratch and Nanoindentation of Deposited and Annealed Nanostructured TiB₂ Based Coatings", *Proceedings the 1st International Conference on Advanced Tribology 2004 (ICAT 2004)*, Singapore.
5. Cunha, L., Moura, C., Leme, J., Andres, G., and Pischow, K., 2004, "Effect of Substrate Bias Voltage on Amorphous Si-C-N Films Produced by PVD Techniques", *Thin Solid Films*, Vol. 447-448, pp. 436-442.
6. Panich, N. and Sun, Y., 2005, "Mechanical Properties of TiB₂-Based Nanostructured Coatings", *Surface Coatings and Technology*, in press.
7. Berger, M., Karlsson, L., Larsson, M., and Hogmark, S., 2001, "Low Stress TiB₂ Coatings with Improved Tribological Properties", *Thin Solid Films*, Vol. 401, pp.179-186.
8. Ronkainen, H., Vihersalo, J., Varjus, S., Zilliacus, R., Ehrnsten, U., and Nenonen, P., 1997, "Improvement of a-C:H Film Adhesion by Intermediate Layers and Sputter Cleaning Procedures on Stainless Steel, Alumina and Cemented Carbide", *Surface Coatings and Technology*, Vol. 90, pp. 190-196.
9. Oliver, W. C. and Pharr, G. M., 1992, "An Improved Technique for Determining Hardness and Elastic Modulus using Load and Displacement Sensing Indentation Experiments", *Journal of Materials Research*, Vol. 7, pp. 1564-1583.
10. Xia, J., Li, X., Dong, H., and Bell T., 2004, "Nanoindentation and Nanoscratch of Thermal Oxide Layer on FeAl Alloy", *Journal of Materials Research*, Vol. 19, pp. 291-300.
11. Holleck, H., 1986, "Material Selection for Hard Coatings", *Journal of Vacuum Science and Technology A*, Vol. 4, pp. 2661-2669.

